

# Diffusion coefficient and acceleration spectrum from direct measurements of charged cosmic ray nuclei

Antonella Castellina<sup>a,d</sup> and Fiorenza Donato<sup>b,d,c</sup>

<sup>a</sup>*Istituto di Fisica dello Spazio Interplanetario, INAF, Torino - Italy*

<sup>b</sup>*Max-Planck Institut für Physik, Munich - Germany*

<sup>c</sup>*Dipartimento di Fisica Teorica, Torino - Italy*

<sup>d</sup>*INFN, Sezione di Torino - Italy*

---

## Abstract

We discuss the potentials of several experimental configurations dedicated to direct measurements of charged cosmic ray (CR) nuclei at energies  $\gtrsim 100$  GeV/n. Within a two-zone propagation model for stable CRs, we calculate light primary and secondary nuclei fluxes for different diffusion and acceleration schemes. We show that the new detectors exploiting the long and ultra long duration balloon flights could determine the diffusion coefficient power index  $\delta$  through the measurement of the boron-to-carbon ratio with an uncertainty of about 10-15 %, if systematic errors are low enough. Only space-based or satellite detectors will be able to determine  $\delta$  with very high accuracy even in the case of important systematic errors, thanks to the higher energy reach and the less severe limitations in the exposure. We show that no uncertainties other than those on  $\delta$  affect the determination of the acceleration slope  $\alpha$ , so that measures of light primary nuclei, such as the carbon one, performed with the same experiments, will provide valuable information on the acceleration mechanisms.

*Key words:* Cosmic rays, Propagation models, Direct measurements

*PACS:* 95.30.-k, 96.40.-z, 96.40.De, 98.70.Sa

---

## 1 Introduction

Charged particles arriving at Earth with energies between about  $10^7$  eV and  $10^{15}$  eV are believed to have galactic origin. Their acceleration is very likely due to the action of supernova remnants, while their subsequent diffusion in the Galaxy is driven by the turbulent, irregular component of the galactic magnetic field. The

most abundant galactic cosmic ray particles have energies in the 100 MeV/n - 10 GeV/n range, where several additional phenomena such as electromagnetic energy losses, convection, diffusive reacceleration and solar modulation are believed to contribute in shaping their spectra. The most realistic description of CR propagation is given by diffusion models, in which the several free parameters inherent to a specific model need to be fixed by observations.

The low-energy tail of the CRs spectrum is shaped by several competing effects, so that it is very difficult to disentangle each physical component. On the other hand, most data have been collected for energies  $\lesssim 50$  GeV/n and their interpretation has not yet led to a clear understanding of any of the above-mentioned physical ingredients. The high energy part of the spectrum - let's say  $\gtrsim 10^2$  GeV/n - is basically due to acceleration and diffusion, all the other effects being minor if not negligible. The best-founded assumptions on the diffusion coefficient and the injection spectrum are power-laws, and this is what is grossly observed for the flux of nuclei.

A wealth of experimental measurements are available, with different degrees of accuracy in the region up to 100 GeV/n; on the contrary, the higher energy region is poorly known. The most recent direct measurements in this region have been provided by the series of balloon flights of JACEE [1] and RUNJOB [2], while most of the data results from indirect measurements, by means of ground arrays observing air showers.

New data have recently been added by the ATIC Collaboration [3], connecting the lowest energy region to the highest energy available data. The new CREAM project [4] has been developed and is now in data taking phase, with the aim of dramatically increasing the available statistics in the energy region up to 500 TeV and possibly more, thus making new and precise measurements of the spectral characteristics of CRs.

In the present paper, we explore the performances required for new detectors to disentangle the fundamental parameters describing the propagation of nuclei at energies above about 100 GeV/n and below the knee region. In Sect. 2 we report on the status of experimental projects aimed at the measurement of CR nuclei at energies  $\gtrsim 1$  GeV/n. In Sect. 3 we describe a diffusion model for galactic CRs, and highlight the main features affecting the propagation of particles in the higher energetic range. Sect. 4 summarizes the method employed for the simulation of the experimental conditions. In Sect. 5 we present our results focusing on the possibilities to measure the diffusion coefficient slope by means of the boron-to-carbon (B/C) data and the acceleration spectrum by means of primary light nuclei fluxes such as the carbon one. In Sect. 6 we draw our conclusions.

## 2 Experimental status and projects

In Table 1, we collected the past and current experiments as well as new projects directly measuring charged CRs nuclei in the energy range above 1 GeV/n and spanning a wide range in  $Z$ .

Direct measurements of charge and energy of CR nuclei started in the sixties, exploiting the balloon and spacecraft techniques. Scintillators and Cerenkov detectors

Table 1

*Balloon and space instruments and new projects. Experiments covering an energy range below 1 GeV/n are not considered in the Table. For all the new projects on satellite we assume 1000 days of data recording. At least 10 events are expected to be detected by ATIC, CREAM and ACCESS above the maximum quoted energy.*

Experiment	Years	Elements	Energy GeV	$\Gamma$ m <sup>2</sup> sr	Exposure (m <sup>2</sup> sr days)
<b>Balloon instruments</b>					
MUBEE [12]	1975-87	$1 \leq Z \leq 26$	$10^4-3 \cdot 10^5$	0.6	22
SANRIKU [13]	1987-91	$8 \leq Z \leq 26$	$2 \cdot 10^2-3 \cdot 10^4$	4.81	4.45
JACEE [1]	1979-95	$1 \leq Z \leq 26$	$2 \cdot 10^3-8 \cdot 10^5$	2-5	65-107
RUNJOB [2]	1995-99	$1 \leq Z \leq 26$	$10^4-3 \cdot 10^5$	1.6	43
TRACER [14]	2002-04	$5 \leq Z \leq 28$	$1.6 \cdot 10^2-1.6 \cdot 10^4$ <sup>1</sup>	5	70
ATIC [3]	2000-03	$1 \leq Z \leq 28$	$10-10^5$	0.25	3.5
CREAM [4]	2004→	$1 \leq Z \leq 28$	$10^3-10^6$	0.5/1.3 <sup>2</sup>	35-140 <sup>3</sup>
<b>Space instruments</b>					
PROTON 1-4 [10]	1965-68	All particles,p,He	$100-10^6$	0.05-10	5-2000
SOKOL [16]	1984-86	$1 \leq Z \leq 26$	$2 \cdot 10^3-10^5$	0.026	0.4
HEAO-3 [11]	1979-80	$4 \leq Z \leq 28$	$9.6-560$ <sup>1</sup>	0.14	33
CRN [17,18]	1985	$4 \leq Z \leq 26$	$7 \cdot 10^2-3 \cdot 10^4$	0.1-0.5/0.5-0.9 <sup>2</sup>	0.3-3
<b>Projects</b>					
NUCLEON-KLEM [19]		$1 \leq Z \leq 26$	$10^2-10^7$	0.19	190
AMS-02 [26]		$1 \leq Z \leq 26$	$1-10^4$	0.5	500
ACCESS [23]		$1 \leq Z \leq 28$	$10^3-5 \cdot 10^6$	1/8 <sup>2</sup>	300-8000
PROTON 5 [20]		$1 \leq Z \leq 28$	$10^3-10^7$	18	18000
INCA-CSTRD [21]		$1 \leq Z \leq 28$	$10^5-10^7$	48	48000

(1) the energy range refers to oxygen;

(2) the two numbers refer to low and high Z respectively;

(3) CREAM had a succesful 40 days flight in December 2004-January 2005, but it is planned to exploit ULDB flights of  $\simeq 100$  days in the near future.

were employed for charge measurement, while ionization calorimeters measured the nucleus energy [5,6,7,8,9,10,11].

Four experiments [1,2,12,13] exploited passive detectors like nuclear emulsions and X-ray films: due to their sensitivity also to inclined tracks, they allowed to reach a much bigger exposure compared to active detectors, thus in principle exploring the highest energy region (about 10 to 1000 TeV). The most precise measurements on relative abundances of elements with Z from 4 up to 28 came from the HEAO-3 mission, whose data have been extensively used to tune and check models. AMS-01 (a spectrometer flown on the space shuttle Discovery including a permanent magnet, a tracker, time-of flight hodoscopes and a Cerenkov counter) brought further information on proton and helium up to about 100 GeV/n [15].

Among the present experiments, a fully active bismuth germanate (BGO) calorime-

ter flew on ATIC [3], while TRACER [14] employed a transition radiation detector. The development of the Long Duration technology is now giving the possibility to balloon experiments to fly for more than 20-30 days, thus reaching much higher exposures. CREAM [4] employs for the first time both a calorimeter and a transition radiation detector, thus allowing an intercalibration of the energy measurement with two independent techniques with different systematic biases. This apparatus is planned to exploit the Ultra Long Duration Balloon flights technology, which relies on new superpressure closed balloons with a pumpkin-shape design and is now in test phase; it will hopefully fly up to 100 days.

New space instruments have also been proposed: a) the NUCLEON russian satellite program which will include the KLEM detector (silicon microstrips and scintillator strips) [19]; b) a ionization calorimeter on a series of Proton-5 satellite missions [20], with the aim of measuring the spectrum of elements up to more than 1000 TeV, reaching an accuracy of 2-5% in the slope determination; c) INCA [21], a ionization neutron calorimeter with 48 m<sup>2</sup>sr acceptance; its main aim being the study of the electron spectrum, it is expected to measure also primary nuclei in the knee region. A proposal for an integration of this calorimeter with a Compton scatter transition radiation detector has been recently presented [22]. The ACCESS [23] project was not chosen for the last MIDEX phase by NASA, but has been included in the hope of a reposition as a free-flyer.

We should also mention the sophisticated spectrometers which were flown on balloons, with the main aim of measuring antimatter and light isotopes [24]. They are not included in the Table because of their quite different aim, but they also gave very precise information on the proton and helium flux up to around 100 GeV/n; the energy range has been extended by the Bess-TeV [25] upgrade of Bess-98, reaching about 500 GeV and 200 GeV/n for proton and helium nuclei respectively. The new AMS-02 [26] large acceptance magnetic spectrometer has been conceived to study origin and structure of the dark matter and to measure antinuclei; it will also be able to extend the knowledge on the composition of charged CRs from the 100 MeV/n region up to about 1 TeV/n.

### 3 Propagation of CRs in the Galaxy

Despite scarce theoretical and observational knowledge of the key parameters responsible for acceleration and propagation of galactic CRs, phenomenological models able to reproduce data can be built. The most realistic propagation models are the diffusion ones, even if the so-called leaky box model has been often preferred in the past for its simplicity [27]. In Refs. [28,29], a two-zones diffusion model has been developed and shown to reproduce several observed species in the low-energy part of the CR spectrum ( $\sim 0.1$ -100 GeV/n). In this model, the Galaxy has been cylindrically shaped (with  $R=20$  kpc), with a thin disc (half-height  $h=0.1$  kpc) containing the sources and the interstellar medium (ISM) surrounded by a diffusive halo of half-thickness  $L \sim 2$ -15 kpc. The transport equation for the nucleus  $j$  in a diffusion model is in principle valid in a very wide range of energies and can be written as:

$$\begin{aligned}
& K(E) \left( \frac{\partial^2}{\partial z^2} + \frac{1}{r} \frac{\partial}{\partial r} \left( r \frac{\partial}{\partial r} \right) \right) N^j(E, r, z) - V_c \frac{\partial}{\partial z} N^j(E, r, z) \\
& + 2h\delta(z) \left( q_0^j Q_j(E) q(r) + \sum_{k=1}^{j-1} \Gamma^{kj} N^k(E, r, 0) - \Gamma^j N^j(E, r, 0) \right) \\
& = 2h\delta(z) \frac{\partial}{\partial E} \left\{ b^j(E) N^j(E, r, 0) - d^j(E) \frac{\partial}{\partial E} N^j(E, r, 0) \right\}
\end{aligned} \tag{1}$$

Steady-state has been assumed and  $N^j(E, r, z)$  is the differential density of the nucleus  $j$  as a function of energy  $E$  and galactic coordinates  $(r, z)$ . In this equation, the first term represents spatial diffusion with diffusion coefficient  $K(E)$ , which has been assumed to be independent of Galactic coordinates.  $V_c$  is the convection velocity, assumed here to be constant throughout the Galaxy (except in the thin disk) and to be directed outward along the  $z$ -direction. The term proportional to  $2h$  in the left-hand side of Eq. (1) takes into account all the sources of cosmic rays: primary sources with injection spectrum  $Q^j(E)$ , secondary spallation production from heavier nuclei and destructive reactions (radioactive-decay terms have been omitted for simplicity). The right-hand side of Eq. (1) contains – through the coefficients  $b^j(E)$  and  $d^j(E)$  – the terms responsible of the energetic changes suffered by charged particles during propagation: Coulomb, ionization and adiabatic expansion losses, and gains due to second order reacceleration. Diffusive, or continuous, reacceleration is due to the scattering of charged particles on the magnetic turbulence in the interstellar hydrodynamical plasma. The diffusive reacceleration coefficient is related to the velocity of such disturbances, called the Alfvén velocity  $V_A$ , and is naturally connected to the space diffusion coefficient  $K(E)$ . For example, diffusive reacceleration contributes significantly in shaping the boron-to-carbon (B/C) ratio at kinetic energy per nucleon  $E$  around 1 GeV/n. Indeed, all energy losses and gains are effective only in the low-energy tail of the CR spectrum and thus are irrelevant in the analysis carried in the following of our paper, which deals with  $E \gtrsim 100$  GeV/n. The so-called sporadic, or distributed, reacceleration has been considered in the literature [30,31] and is based on the possibility that CRs be reaccelerated during their wandering in the Galaxy by supernova remnants (SNRs) and gain a small amount of energy at each encounter.

Convection may dominate at low energies, depending on the value of  $V_c$  and if  $\delta$  is large. It may compete with diffusion up to few tens of GeV/n, but its role becomes negligible at higher energies. The importance of spallation processes depends on the nucleus, but at energies  $\gtrsim 100$  GeV/n they are not much relevant except for heavy nuclei (e.g. iron) [32]. We also note that the different assumptions on the distribution of the ISM – homogeneously distributed (as assumed in our analysis) or spatial dependent – are irrelevant at high energies and for the species considered in our analysis.

Diffusion depends on the rigidity  $R$  ( $R = p/Z$ ) of the particle and the diffusion coefficient is usually assumed to have the form:  $K(E) = K_0 \beta R^\delta$ .  $K_0$  is linked to the level of the hydromagnetic turbulence and  $\delta$  to the density spectrum of these irregularities at different wavelength. The Kolmogorov theory for the turbulence spectrum predicts  $\delta=1/3$ , while the case for a hydromagnetic spectrum with  $\delta=1/2$  has been obtained by Kraichnan [33]. On the other side, the phenomenological interpretations of CR spectra have not led to fix  $\delta$  because of the complicated treatment

of the physical phenomena which are relevant at the energies in which most cosmic particles have been collected. Fits to the B/C ratio within the diffusion model of Eq. (1) prefer high values for  $\delta$  ( $\sim 0.5-0.75$ ), while the Kolmogorov spectrum turns out to be disfavored [28,29,34]. The  $\delta=1/3$  case can reproduce quite well the peculiar B/C peak observed at  $\sim 1$  GeV/n but it tends to overestimate the data at increasing energies, predicting a quite flat B/C ratio (see also later). The highest values of  $\delta$  seem on the other side not very realistic. In fact they are only marginally consistent with observations of interstellar scintillation [35,36] and are highly incompatible with the level of anisotropy measured at 1-100 TeV [37]. Data on CR fluxes do not extend to sufficiently high energies and are not sufficiently precise in order to constrain  $\delta$ .

The acceleration spectrum of primary CRs is believed to be determined by supernovae (SN) remnants and super-bubbles [38], which are the only known engines in the Galaxy able to provide the right amount of energy to particles up to  $\sim Z \times 10^{14}$  eV. The acceleration spectrum follows a power-law in momentum,  $Q(E) \propto p^{-\alpha}$ , with  $\alpha$  located somehow between 2.0 and 2.5. Even if a precise value for  $\alpha$  cannot be predicted, the effective spectral index as derived by several indirect observational tests and by numerical studies is close to  $\alpha \sim 2.0-2.1$  [38] (and refs. therein), [39]. Very recently, the TeV  $\gamma$ -ray image of a SN remnant - already observed in the X-ray spectrum with a very similar morphology - strongly indicates that high energy nuclei are accelerated in this site [40]. The  $\gamma$ -ray data are well reproduced by a photon spectral index which seems to prefer low  $\alpha$  values, even if the experimental sensitivity is not yet sufficient to put strong constraints. Higher values of  $\alpha \sim 2.4$  are favored by propagation models for GCRs with very low  $\delta$ , such as the Kolmogorov spectrum.

The above-described diffusion model has been tested on the B/C and sub-Fe/Fe ratios and shown to fit well existing data, which we remind lie in the low-energy tail of the galactic CR spectrum [28,29]. The propagation parameters able to reproduce such ratios give also rise to a secondary antiproton flux which is in very good agreement with measurements [41]. A further, yet weaker, degree of consistency is given by an analysis of radioactive isotopes [42]. In this case, the diffusion model has been modified in order to take into account a local under-dense region, relevant when dealing with short-living species. The model has also been validated at higher energies through a study of the mean logarithmic mass of the CR [32] beam. For further details on this propagation model and considerations on other possible approaches we refer to Ref. [43] and references therein.

## 4 Detector design and simulation

To pursue the objective of extracting information about crucial propagation parameters in the high energy region, an experimental apparatus should have the following characteristics:

- (i) A large exposure, to have enough statistics: to detect about 10 nuclei at energies above 10 TeV/n, if taking the elemental fluxes from [44], a collecting power  $\Gamma \simeq 53$  m<sup>2</sup>sr days is to be reached for carbon nuclei, while more than 250 m<sup>2</sup>sr days are

necessary for Iron.

(ii) A good energy resolution: this is especially crucial to detect changes of slope in the energy spectra (e.g. the knee in the proton spectrum) or to study spectral smoothness. A constant 40% energy resolution is enough to see an increase in the spectral slope of about 0.3 crossing the knee. The same resolution or better is required to find small deviations from smoothness, of the order of 10% [20].

(iii) A charge resolution such as to distinguish e.g. carbon from boron nuclei; models ask for a B/C ratio of some percent around 1 TeV/n, so that a resolution of about 0.2 charge units is needed.

Combining different detectors in the same experiment gives a powerful tool to overcome individual technical limitations: for example, redundant measurements of energy allow a cross-calibration of the detectors, thus overcoming the problem of direct energy calibration which at the highest energies explored is possible for TRDs but not for calorimeters.

A very careful study of systematic errors is mandatory, as these are the main cause of uncertainty in all the measurements. Exposures and efficiencies in selecting and tracking the events can be studied by means of Monte Carlo simulations; for both energy and charge determination, redundancy can help in reducing the ambiguities. Although a serious discussion of systematics depends on each specific detector, a constant contribution to the overall error on the flux measurements will be introduced in our analysis.

In order to explore the performances of new detectors, a simulation has been built with the following ingredients:

(a) the input flux; the particle spectrum is numerically given by the propagation model. Different power laws with increasing slope in contiguous energy ranges are fitted to the spectrum to better follow the expected behavior. The flux is normalized to the best experimental low energy datum (e.g. the flux as derived by [11] at 10.6 GeV/n).

(b) the experimental apparatus, in terms of collecting power and energy resolution. We use  $\Gamma = 1.3, 5$  and  $10 \text{ m}^2\text{sr}$ , similar to the quoted geometrical factors of some of the current and future experiments and a set of exposure times of 30, 100 and 1000 days, which roughly correspond to long and ultra long duration balloon flights and satellite conditions, respectively.

The expected number of events above a given energy  $E$  for an assumed collecting power  $\Gamma$  and input spectrum  $dN/dE = C_0 E^{-\gamma} \text{ m}^{-2}\text{s}^{-1}\text{sr}^{-1}(\text{GeV}/n)^{-1}$  can be written as:

$$N(> E) = \Gamma C_1 E^{-\gamma+1} \quad (2)$$

where  $C_1$  depends on the slope and normalization of the input flux.

Following the approach of [45], the cumulative distribution function for  $E$  in the considered energy range can be written as

$$\Phi(E) = 1 - \frac{N(> E) - N(> E_b)}{N(> E_a) - N(> E_b)} \quad [E_a \leq E \leq E_b] \quad (3)$$

and the probability distribution function for the events is obtained by differentiation

$$d\Phi(E)/dE = \frac{(\gamma - 1)}{E_a^{-\gamma+1} - E_b^{-\gamma+1}} E^{-\gamma} \quad (4)$$

The number of events  $N$  of Eq.2 is the mean value of the Poisson distribution of the true number of events in a given range  $[E_a - E_b]$ ; the poissonian fluctuation is computed in small energy bins (equal bins in logarithmic scale so that, for any interval  $j$ ,  $E_{j+1}/E_j = \text{constant}$ ) covering the full interval, in order to correctly weight also the bins with few events. The energy of each  $i$ -th event is then randomly sampled in the energy interval  $[E_a - E_b]$  from the power law spectrum; being  $r_i$  a standard uniform variate

$$\Phi(E_i) = \int_{E_a}^{E_i} d\Phi(E')/dE' dE' = r_i \quad (5)$$

and

$$E_i = \{r_i(E_b^{-\gamma+1} - E_a^{-\gamma+1}) + E_a^{-\gamma+1}\}^{\frac{1}{1-\gamma}} \quad (6)$$

In each interval  $[E_j - E_{j+1}]$ , the mean energy is

$$\langle E \rangle = \left(\frac{\gamma}{\gamma - 1}\right) \left(\frac{E_j^{-\gamma+1} - E_{j+1}^{-\gamma+1}}{E_j^{-\gamma} - E_{j+1}^{-\gamma}}\right) \quad (7)$$

The detector response is modeled as a Gaussian distribution with mean equal to the input energy and width given by the energy resolution. In the following, a constant 40% energy resolution will be assumed; the case for resolutions either decreasing or increasing with energy will however be checked. The detection efficiency is here assumed not to depend on energy and will be included in the systematic uncertainties.

## 5 Results and discussion

The aim of this section is to study the potentials of different experimental configurations in connection with the determination of the diffusion coefficient slope  $\delta$  and the acceleration power spectrum  $\alpha$ . We show how well their physical value could be singled out with high-energy data on the B/C ratio and the carbon flux.

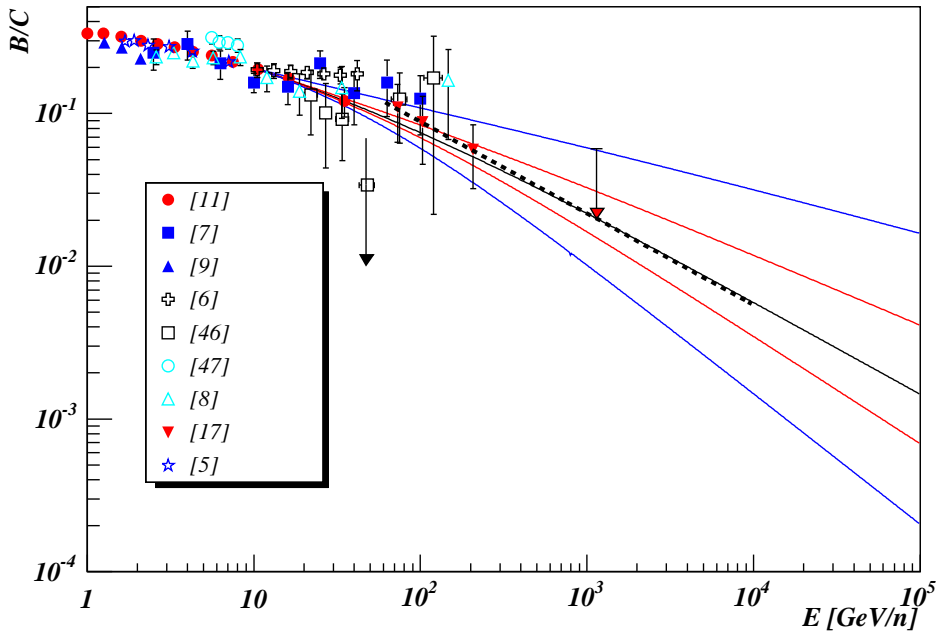


Fig. 1.  $B/C$  ratio as a function of kinetic energy per nucleon. Solid curves: theoretical predictions corresponding, from top to bottom, to cases 1-2-3-4-5, respectively (see text for details). Dashed line: simple power law spectrum  $B/C=1.4 E^{-0.60}$ .

### 5.1 $B/C$ and the diffusion coefficient slope

The boron-to-carbon ratio has always been considered the best quantity to study diffusion properties. At energies around GeV/n, this ratio is strongly affected by the low-energy phenomena described in Sect. 3. In particular, the observed bump at  $\sim 1$  GeV/n can be naturally explained by diffusive reacceleration, without invoking any artificial break in the diffusion coefficient.

The most precise  $B/C$  data have been obtained in the energy range 0.6-35 GeV/n by the HEAO-3 experiment [11], the highest energy points having been collected by CRN [17]. In Fig. 1 we plot a collection of data on the  $B/C$  ratio giving emphasis to the higher energy part of the spectrum. Along with the experimental data, we also plot the theoretical predictions calculated with the full diffusion model briefly outlined in Sect. 3.

We have chosen five illustrative configurations of the propagation parameter space, which will be also employed in the following of our analysis as bench marks. At the energies we deal with, the parameter which mostly shapes the  $B/C$  ratio is the diffusion coefficient slope, namely  $\delta$ . The constant  $K_0$  in the diffusion coefficient enters with the source abundances in the global normalisation of  $B/C$ , so that its precise value is of scarce relevance in the  $B/C$  predictions. We thus identify cases 1-2-3-4-5 with  $\delta = 0.3, 0.46, 0.6, 0.7, 0.85$ , respectively. All the other propagation parameters ( $K_0, L, V_c, V_A, \alpha$ ) have been fixed according to the best fits to  $B/C$  data [29]. Indeed their exact value is not very important when working with a secondary-to-primary flux ratio at energies  $\gtrsim 100$  GeV/n. The dashed line in Fig.1 corresponds

to the power law  $1.4E^{-0.60}$ , where the coefficient 1.4 has been fixed to the theoretical prediction for the  $\delta=0.6$  case at 1000 GeV/n. This line shows that for energies  $\gtrsim 1000$  GeV/n the B/C ratio can be well approximated by a power law in energy with index  $-\delta$ , as one expects from the high energy limit: secondary/primary  $\propto K(E)^{-1} \propto R^{-\delta}$ . At  $E=100$  GeV/n the difference between the simple power law and the calculated flux is  $\lesssim 20\%$ . Below this energy, it is clear that the effects of energy changing, convection, halo size and spallations become more and more important in shaping the B/C ratio, as studied in Refs. [28,29].

This figure wants to emphasize the discrepancy among the models - basically due to the  $\delta$  values - with increasing energy. At energies  $\sim 100$  TeV/n the predictions for B/C ratio in the  $\delta=0.3$  and  $\delta=0.85$  case - both not excluded by low energy data, even if  $\delta=0.85$  is a quite extreme value - differ by two orders of magnitude. Different predictions for  $\delta$  lead to B/C whose relative values increase with increasing energy. This high energy region is thus very interesting from an experimental point of view, since it could bring - at least in principle - to a clear determination of the actual diffusive regime.

Finally, we want to underline that the injection spectrum has no relevance in the calculation of this ratio. We have checked that for  $E \gtrsim 10$  GeV/n the results for the B/C ratio are practically unchanged if we vary  $\alpha$  (equal for each nucleus) in the very large range 1.8-2.5, as well as if we fix  $\alpha$  for each nucleus ( $\alpha^j$ , indeed) as derived in Ref. [44].

Following the procedure outlined in Sect. 4, the expected number of carbon and boron events can be derived by selecting a given set of experimental conditions (exposure, time and resolution) and an input flux. Fig.2 shows the B/C ratio as obtained from case 1 (upper panel, corresponding to  $\delta=0.3$ ) and from case 3 (bottom panel,  $\delta=0.6$ ), for three different collecting powers. The maximum energy at which the B/C ratio can be measured with a significant number of events - we are requiring at least 10 events for Boron nuclei - goes from about 900 GeV/n to more than 10 TeV/n when the exposure increases from about 40 m<sup>2</sup>sr days up to 10000 m<sup>2</sup>sr days. The various correction factors which must be considered in the analysis of real data (e.g. due to selection efficiency or interaction losses in the apparatus) would have the effect of lowering the maximum detectable energy. As an example, a global efficiency of 30% would shift it by a factor 1.5 for the smallest exposure considered here and case 3 as input. The same effect is produced for balloon experiments due to spallation processes in the residual atmospheric grammage of 4-5 g/cm<sup>2</sup>.

From this figure it is evident that the two theoretical models could be easily distinguished already by experiments with acceptance of about 1 m<sup>2</sup> sr and flying time of forty days (in our example: 1.3 m<sup>2</sup> sr and 30 days data taking). Note however that the figure has been obtained without considering the systematic uncertainties. The inclusion of a finite energy resolution of the detector in the simulation has important consequences on the ability to measure the B/C ratio and to distinguish among different models: it produces in fact a distortion which reflects the change in the carbon and (more) in the boron spectra due to the energy fluctuation. The steepness of the spectra makes it more likely to move low energy events to high energy bins, so that the effect is bigger for weaker spectra. In the case of model 1, for example, the measured B/C will be some percent higher than what expected for

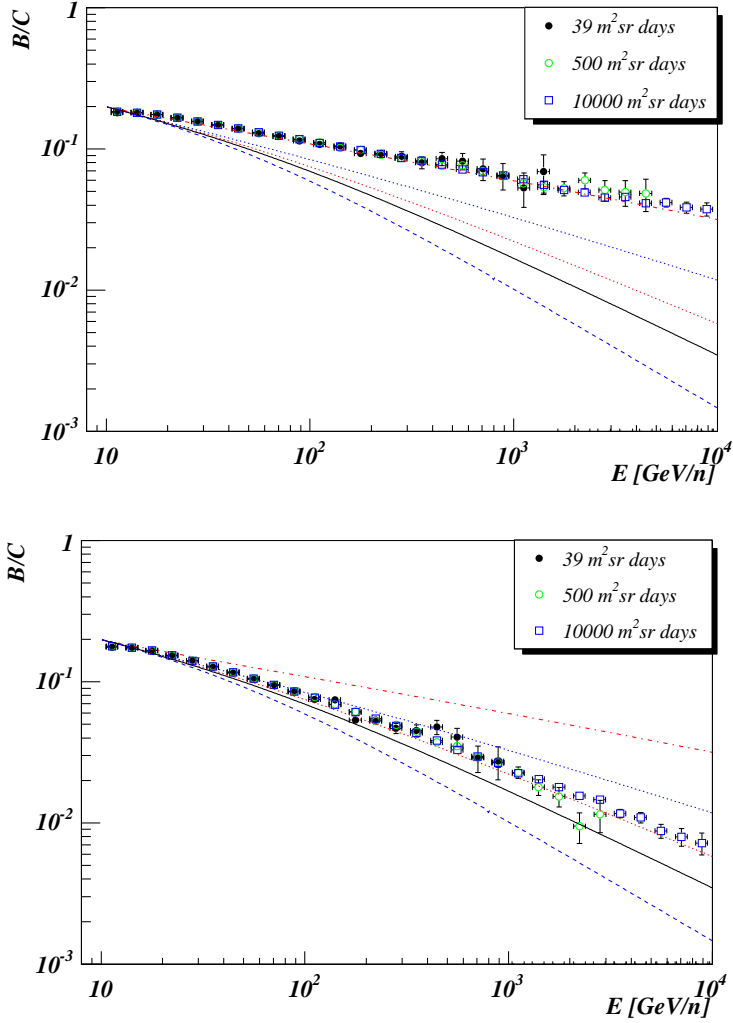


Fig. 2.  $B/C$  ratio as expected from input case 1 (upper panel) and 3 (lower panel) for different experimental exposures. The expected ratios from cases 1 to 5 (from top to bottom, respectively) are also shown.

an ideal detector, that is a “zero resolution” one, almost constantly from 100 GeV/n on; on the contrary, using the input spectrum of model 5 the  $B/C$  ratio appears to be from 12 to 18% higher when going from 100 to 1000 GeV/n. A correction for this effect has to be applied before the comparison with expectations; the binning of the data should be carefully chosen in order to be bigger than the uncertainty due to energy resolution.

Using two different input models  $j$  and  $k$ , we simulated the expected number of carbon and boron events. The difference between the  $B/C$  ratios so derived can be quantified by performing a relative  $\chi^2$  test

$$\chi^2 = \sum_i \frac{((B/C)_{ij} - (B/C)_{ik})^2}{\sigma_{ij}^2 + \sigma_{ik}^2} \quad (8)$$

where we put at denominator the variance of the difference. In order to fully exploit the high energy region which can be explored by the current and future apparatus, where only acceleration and diffusion dominate the cosmic rays spectrum, the summation starts from 100 GeV/n.

The ratio between the carbon and boron fluxes is only mildly sensitive to systematic errors (most of which are supposed to be independent from the considered nucleus), which are however to be included in the total error. Since a full discussion on systematics can only be done for each specific apparatus, we consider here only a constant systematic error to be added in quadrature to the statistical one.

Fig.3 shows the result for the data sets respectively expected from model 3 and each of the other ones as a function of the systematic uncertainty, for three different experimental collecting powers. We should remind that even at the lowest energy of 100 GeV/n the percentage difference between models is big, going from about 7% for models 3 and 4 up to 30% for models 1 and 2. Exposures are such that even for the smallest experimental configuration considered here the statistical errors are quite small and in the ideal case of no systematic effects all models could be separated. As obvious, the sensitivity increases with differences between the two compared  $\delta$  values, in our case the ones labeled (1-3) and (3-5) for which  $(\delta_j - \delta_k)=0.30$  and  $0.25$  respectively. For example, a  $\delta=0.3$  case can be distinguished from a  $\delta=0.6$  case with 90% C.L. if the systematic error stays below 12% even in the less favourable experimental conditions considered. In the case of a satellite-like exposure, these two models could be distinguished even in presence of a 15% systematic error. On the other hand, the range of sensitivity raises up to more than 20 TeV/n for satellite-based experiments, thus allowing to tag bench marks with  $\Delta\delta=0.10-0.15$  (e.g. case 2 from 3 or case 3 from 4), but only if systematic uncertainties are kept below 10%.

The analysis shown in Fig.3 is meant to illustrate the ability of a given experimental setup to discriminate between two fixed and arbitrarily chosen  $\delta$  values. In order to evaluate the accuracy in the determination of  $\delta$ , we now perform a  $\chi^2$  minimization procedure on the simulated B/C data, leaving  $\delta$ ,  $K_0$ ,  $L$  and  $V_c$  as free parameters. As expected, the resulting  $\chi^2$  has no structure with respect to  $K_0$ ,  $L$  and  $V_c$ , whose effect is in practice reabsorbed in a global normalization of the spectra. On the contrary, the calculated  $\chi^2$ s are such that a minimum for  $\delta$  can always be clearly identified.

If systematics can be considered negligible, the determination of the diffusion coefficient slope can be obtained at 10-15% significance from B/C data collected with the 39 m<sup>2</sup> sr days simulated experiment, and at 8%-10% for the 500 m<sup>2</sup> sr days case. However, we find that  $\delta$  can be determined with significance level of 15% or 10% respectively for the 500 m<sup>2</sup> sr days or 10000 m<sup>2</sup> sr days simulated experiment, if the systematic errors are of order 10%. Very low accuracy is predicted in this case from the lowest exposure experiment (39 m<sup>2</sup> sr days).

As expected, the obtained accuracies are consistent with the probability curves shown in Fig.3; e.g., the case 3-4 presented in this figure (bottom left) considers two  $\delta$  differing by 15-20% and shows that they are perfectly separated only if the systematic uncertainties lay below 2-3% for the smallest collecting power. This agrees with our previous conclusion, namely that the accuracy on  $\delta$  is at the level of 10% for a collecting power of 39 m<sup>2</sup> sr day and negligible systematics.

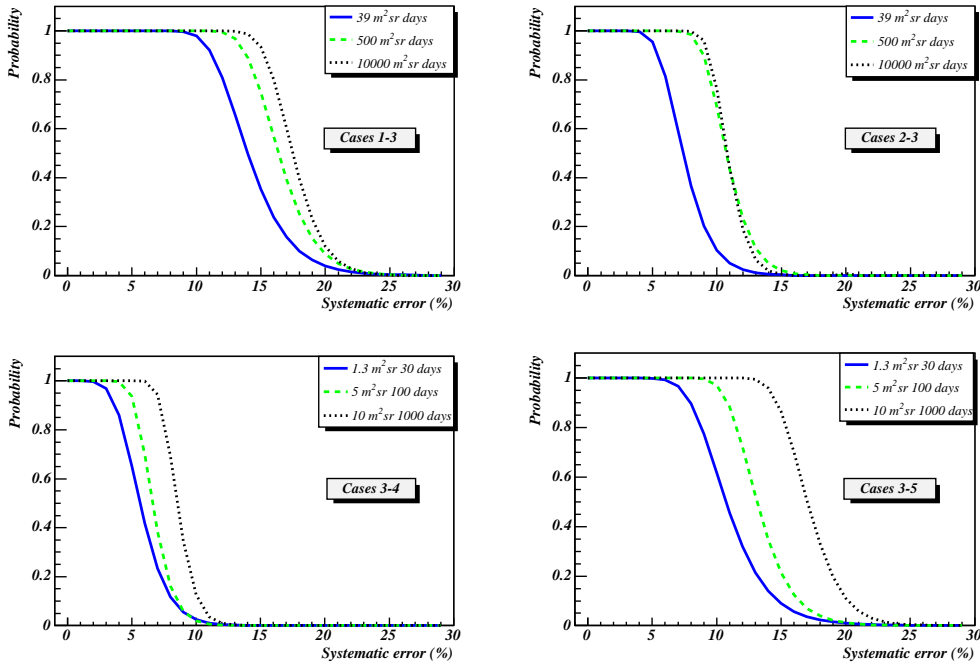


Fig. 3. Probability of distinguishing between two input models vs systematic error for three different collecting powers. Remind that, for cases 1-5,  $\delta=0.30, 0.46, 0.60, 0.70, 0.85$  respectively.

We emphasize once again that the above results are derived including systematic uncertainties which are assumed to be independent on energy: while this is true for trigger efficiency or event reconstruction, or even for Monte Carlo corrections, other systematic errors like those due to energy resolution will depend on energy and could alter the considered fluxes.

A spectral deformation of the B/C ratio at high energies has been proposed in Ref. [31] as due to distributed reacceleration (see above). CR particles can have sporadic encounters with SNRs, during which they could gain small amount of energies. The modification of the primary spectrum comes out to be independent of energy, while the effect for secondaries increases with energy just as the diffusion coefficient in the Galaxy. Thus, the ratio of reaccelerated  $B/C^{re}$  to standard B/C would be roughly described by  $(B/C)^{re} / (B/C) \propto (\alpha + \delta - 1) / (\alpha + 2\delta - 1) (p/p_{GCR})^\delta$ , where  $p_{GCR}$  is the momentum corresponding to the maximum of the observed particle spectrum (in Ref. [31] it is assumed  $E_{GCR}=0.6$  GeV/n). The real situation is rather more complicated than this description, which nevertheless gives us the correct trend and the possible magnitude of the effect. The expected deformation of the B/C ratio would be greater for greater  $\delta$ . Moreover, as figured out in Ref. [31], its intensity would strongly depend on the value of the circumstellar hydrogen density,  $N_H$ . The higher  $N_H$ , the lower the distortion. In the case of  $\delta=0.6$ , an effect of one order of magnitude would be expected at 1 TeV/n for  $N_H=0.003$  cm $^{-3}$ , a very low number, indeed. For higher and more plausible values of the hydrogen density, the B/C ratio could be enhanced by a factor of two. If the diffusion is Kolmogorov-like, only very small  $N_H$  could give an observable effect (about a factor two). But in this case it would be less ambiguous to correctly interpret data, while in case of higher  $\delta$  this

sporadic reacceleration effect could be mimicked by smaller  $\delta$  effects. Non-stationary models have also been studied, taking into account the fact that SN might be considered discrete sources in the Galaxy, so that a time-dependent diffusion equation should be solved [49]. However, it seems plausible that the B/C ration would not be modified in shape, but only in a overall normalization factor [50].

## 5.2 Primary fluxes and acceleration spectra

Primary fluxes trace back to the diffusion and acceleration properties, since they are produced directly in the acceleration sites. Charged CR nuclei heavier than protons suffer catastrophic losses due to nuclear destruction on the interstellar H and He. These reactions become irrelevant on the CR spectrum at energies of about 1 TeV/n, depending on the nuclear species. The effect of inelastic interactions lowers and flattens the flux, giving rise to a final shape that is harder than a pure power-law  $E^{-\gamma}$ , being  $\gamma = \alpha + \delta$ . This effect has been studied by computing the carbon flux

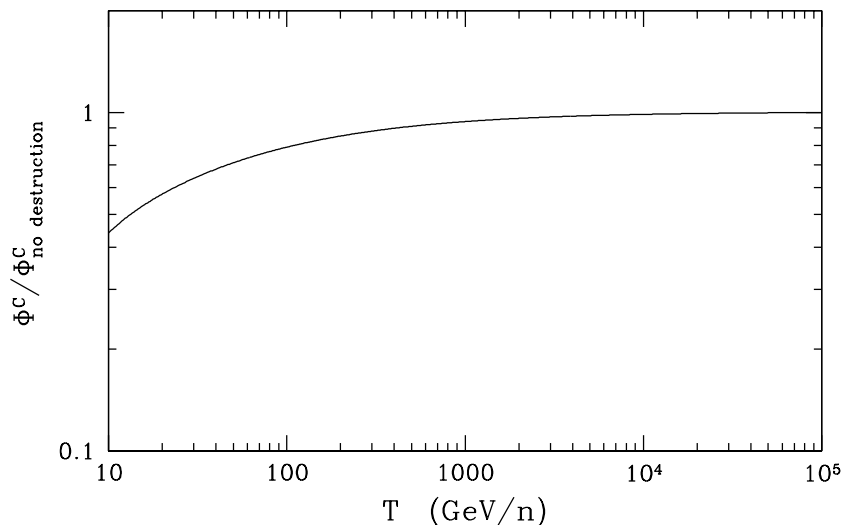


Fig. 4. *Ratio of calculated carbon fluxes from the same propagation model, where nuclear destructions have been turned off at the denominator.*

according to the full diffusion model (case 2 and  $\alpha = 2.05$ , but in this context their value is not relevant) with and without inelastic destructions; the result is plotted in Fig.4 (for iron flux, see Fig. 1 in [32]). The difference between the two cases is about 30% at 100 GeV/n, and at 1 TeV/n it is still 5%. Thus, it is in principle not correct to expect a pure power law spectrum from energies above few tens of GeV/n, as often claimed in literature. Of course, the error bars on the existing experimental data for primaries (except for protons, maybe) still justify this approximation.

From the experimental point of view, data about fluxes of primary nuclei were collected in the past for  $Z \leq 26$  up to few TeV/n, but with decreasing statistical significance as the energy grows higher. At the highest energies, the only available data sets come from emulsion chamber experiments [1,2,16] which measure groups of elements; systematics are quite large, e.g. the results for the CNO group differ between JACEE and RUNJOB by a factor of 2 in normalization. More recently, the first data from a one day test flight of TRACER have been published for  $Z \geq 8$  nuclei [48].

We have calculated the carbon flux for a propagation model in agreement with the B/C analysis presented above, with the only aim to qualitatively reproduce the data at the energies in discussion. So we do not care much about the level of agreement with lower energy data, aware that a thorough study of the propagation of primaries at low energies would require many deeper insights, which are beyond the scope of the present paper. Figure 5 shows a compilation of the data on carbon flux together with the calculated flux for model 3 ( $\delta=0.6$ ) and  $\alpha=1.9, 2.05$  and  $2.2$ . The normalization has an important role in this calculations and may be ascribed to the value of the source abundances, which are very poorly known, and of  $K_0$ . We refer our normalization to the fluxes measured at 35 GeV/n [11], where the total error (statistical and systematic) is about 15%.

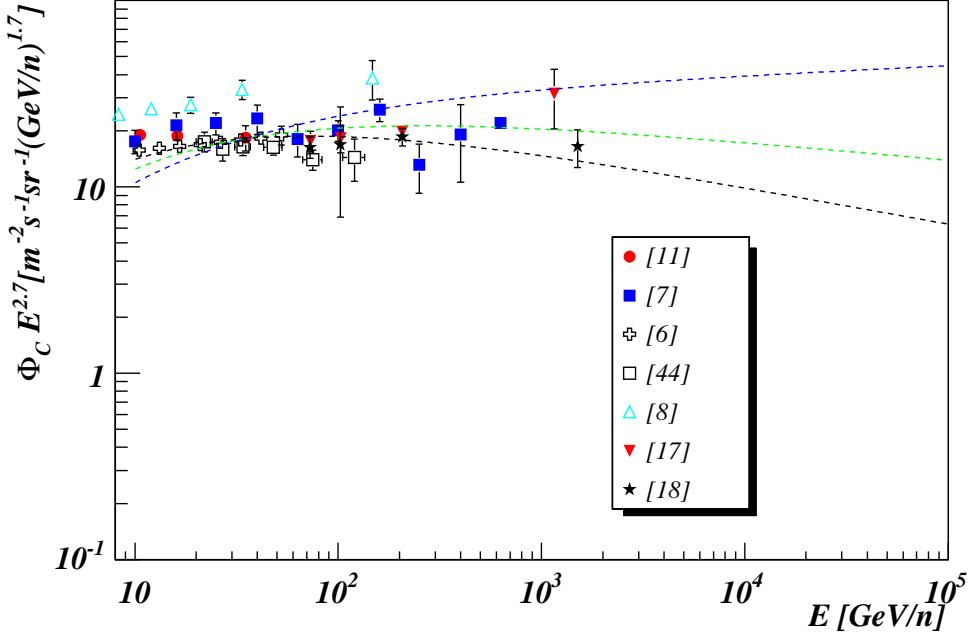


Fig. 5. Data on carbon flux multiplied by  $E^{2.7}$ ; 3 theoretical models are shown, corresponding to  $\delta=0.6$  and  $\alpha=1.9, 2.05, 2.2$  from top to bottom, respectively.

The expected number of events from the above described model and for different values of  $\alpha$  have been calculated following the procedure described in Sect.4 for different experimental exposures; the corresponding flux is shown in Fig. 6.

We have also checked that this flux is almost independent of the assumed energy

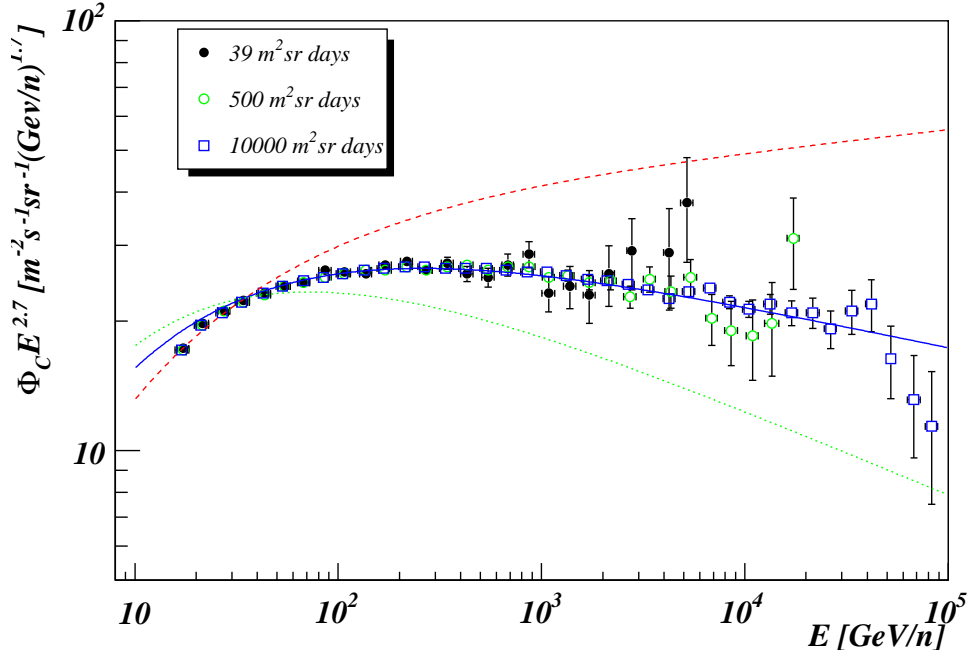


Fig. 6. *Expected C flux for input model with  $\alpha = 2.05$  and  $\delta = 0.6$  and 3 different exposures. Theoretical curves as in Fig. 5.*

resolution by changing it from a constant value to an either decreasing or increasing behavior as a function of the particle energy (from 40% at 100 GeV/n to either 50% or 30% at 1000 GeV/n). Indeed, it can be shown that the energy resolution plays a minor role as compared to the event statistics (to collecting power) in the estimation of spectral slopes for simple power laws [45].

The statistical error on the expected events is less than 2% up to about 500 GeV/n, rising to 10% at 2 TeV/n for the smallest exposure, with 500 m<sup>2</sup>sr days it lowers to few percent at 1-2 TeV/n: the new detectors will so have full ability to cover the high energy range with sufficient statistical precision. With a  $\chi^2$  minimization procedure, the expected data are fitted to a power law and the slope  $\gamma$  is determined with an error lower than 1% in a range  $\Delta E=0.1-10$  TeV/n. The effect of adding a constant systematic error of 10% is of more than doubling the error on  $\gamma$ .

This result implies that the experimental errors on the carbon flux (the same conclusion is reached for oxygen) will not add any uncertainty in the determination of the acceleration power law index  $\alpha$  other than the one carried by the diffusion slope  $\delta$ . If the latter is determined within 10% from B/C measurements, the same experiment will let us fix the former within an equal uncertainty level by means of primary fluxes determination.

The knowledge of  $\alpha$  will lead to a better understanding of the acceleration processes inside galactic supernova remnants. In particular, we note that even in a LDB mission it could be possible to reach 1 TeV/n with quite good statistical accuracy, thus allowing to confirm or exclude whether  $\alpha$  lies towards low-values 1.9-2.1, or in the higher range 2.3-2.4 at a 3  $\sigma$  level.

## 6 Conclusions

A two-zone diffusion model for stable, galactic CRs has been extensively used to generate different predictions on the primary and secondary nuclei fluxes, which in turn are used to evaluate the expected events in various experimental configurations similar to present or next generation apparatus. They will substantially exploit a high collecting power in the high energy region ( $\geq 100$  GeV/n), where the low energy effects and most of the peculiarities of the model can be neglected. We have shown that new detectors exploiting the long and ultra long duration balloon flights, or even more future space missions, will provide valuable information about both the diffusion coefficient slope  $\delta$  and the acceleration spectrum  $\alpha$  of galactic CRs.

An experimental determination of  $\delta$  through the measurement of the B/C ratio is at reach of the new generation of detectors, some of which are already taking data. An experiment like CREAM - which during its first flight collected data for more than 40 days breaking all the previous flight and duration records<sup>4</sup> - is in principle able to distinguish between a Kolmogorov-like or a different turbulent regime, determining  $\delta$  with an uncertainty of about 10-15%, if systematic errors are low enough. If the latter were important and at a level of about 10%, the uncertainties on the derived  $\delta$  would be huge. Experiments reaching collecting powers of hundreds  $\text{m}^2$  sr days have the potential of fixing  $\delta$  at about 85% confidence level even in the case of important systematic errors, or at  $\gtrsim 90\%$  if the latter are of the order of the statistical ones.

Only space-based or satellite detectors will be able to determine  $\delta$  with very high accuracy. In fact, even if they would be affected by not negligible systematic errors, the covered energy range would be significantly wider (we discussed the case with maximal energy of order 30 TeV/n).

A careful measurement of the single fluxes will shed new light on the acceleration spectrum: in the high energy region the new generation apparatus will be able to measure the spectrum slope  $\gamma$  for light nuclei with a negligible error. No further uncertainty other than the one affecting  $\delta$  as derived from the B/C ratio will then be added to the determination of the acceleration slope  $\alpha$ . This last parameter is thus expected to be measured with an uncertainty of 10-15% in the near future, allowing to exclude large ranges of  $\alpha$  values and leading to a much clearer understanding of the acceleration processes.

The spectra of the single elements of the CR beam will be measured with very good statistics up to more than some  $10^{14}$  eV (which is the correct unit to be used when comparing with indirect measurements, for which only the energy/particle is determined). With a careful analysis of the experimental systematics, absolute particle fluxes will be provided, thus giving more than a decade calibration region to the Extensive Air Shower detectors. Direct measurements based on adequate statistics in the region of overlap with the Extensive Air Shower explored region are of main importance in order to give ground based experiments a firm reference point, thus helping in deriving the mean composition of the CR beam towards and at the knee and in checking the models which are used to derive the energy. Around  $10^{14}$  eV, the flux uncertainty can be set at present around 30%; with the new experiments now

---

<sup>4</sup> <http://cosmicray.umd.edu/cream/cream.html>

under way or in project, we can expect to significantly reduce it. The same is true for what regards the mean mass: results from indirect measurements are far from clear [51], while data from direct detection still show about 30% uncertainty above  $10^{14}$  eV, which can surely be lowered at least to 15-20% with the new apparatus.

At high energy, above 100 GeV/n, the primary nucleons contribute mainly to neutrino-induced upward through-going or stopping muons [52]; most important are protons and helium nuclei, while heavier ones contribute less than  $\simeq 10\%$  at all energies. Apparata with the considered exposures will be able to measure also proton and helium spectra with unprecedented accuracy, thus allowing to reduce the present uncertainty in the all nucleon spectrum, which including all the available data is still around 30% in the TeV range.

We want to emphasize that a better understanding of the propagation properties is of great significance for the study of signatures of new physics in CRs. Indirect signals of dark matter pairs annihilating in the halo of our Galaxy could be found in antiproton, antideuteron or positron CRs. This research is limited by the uncertainties in the propagation parameters, that dramatically affect the fluxes of charged particles located in the whole diffusive halo [53]. For instance, if this uncertainty were significantly reduced, it would be possible to exclude supersymmetric models predicting antiproton fluxes exceeding the present measurements [54]. A better signal-background discrimination would come from antideuteron measurements [55], and a reduction of the astrophysical uncertainties on the calculated fluxes would be even more desirable.

We conclude by reminding that important parameters – other than  $\delta$  and  $\alpha$  – describing our Galaxy in relation to the propagation of charged particles can be fixed only with very precise low energies data, and for various species. This in principle could be done by the AMS experiment on the Space Station [26], which could measure fluxes from hundreds MeV/n up to TeV/n and for  $1 \lesssim Z \lesssim 26$ .

## 7 Acknowledgements

We warmly thank D. Maurin and R. Taillet for the usage of numerical code for cosmic ray propagation developed in collaboration with one of the author (F.D.), and M. Aglietta, B. Alessandro, T. Janka, P.S. Marrocchesi, D. Maurin and G. Raffelt for useful discussions. F.D. acknowledges the A. von Humboldt Stiftung for financial support while at MPI in München.

## References

- [1] K.Asakimori et al., ApJ **502** (1998) 278.
- [2] A.V.Apanasenko, Astropart.Phys. **16** (2001) 13.
- [3] H.S.Ahn et al., COSPAR-04; V.I.Zatsepin et al., Proc. 28th Int. Cosmic Ray Conf., Tsukuba, Japan (2003) 1829.

- [4] E.S.Seo et al., *Adv.in Space Res.* **33** (2004) 1777.
- [5] R.Dwyer and P.Meyer, *ApJ* **322** (1987) 981.
- [6] J.A.Lezniak and W.R.Webber, *ApJ* **223** (1978) 676.
- [7] M.Simon et al., *ApJ* **239** (1980) 712.
- [8] C.D.Orth et al., *ApJ* **226** (1978) 1147.
- [9] R.C.Mahel et al., *Ap&SS* **47** (1977) 163.
- [10] N.L.Grigorov et al., *Proc.12th Int.Cosmic Ray Conf., Hobart*, **5**(1971)1746.
- [11] J.J.Engelmann et al., *A&A* **233** (1990) 96.
- [12] V.I.Zatsepin et al., *Proc.23rd Int. Cosmic Ray Conf., Calgary (Canada)* **2** (1993) 13.
- [13] M.Ichimura et al., *Phys.Rev.***D48** (1993) 1949.
- [14] F.Gahbauer et al., *ApJ* **607** (2004) 333.
- [15] J.Alcaraz et al., *Phys.Lett.* **B472** (2000) 215; J.Alcaraz et al., *Phys.Lett.* **B494** (2000) 193.
- [16] I.P.Ivanenko et al., *Proc.23rd Int.Cosmic Ray Conf., Calgary (Canada)* **2** (1993) 17.
- [17] S. P. Swordy et al., *ApJ* **349** (1990) 625.
- [18] D.Müller et al., *ApJ* **374** (1991) 356.
- [19] G.Bahsindzhagyan et al., *Proc.28th Int.Cosmic Ray Conf.,Tsukuba (Japan)* (2003) 2205.
- [20] N.L.Grigorov, *Cosmic Res.* **40**, 2 (2002) 107.
- [21] A.P.Chubenko et al., *Proc. 28th Int.Cosmic Ray Conf., Tsukuba (Japan)* (2003) 2221; R.A.Mukhamedshin et al., *Proc. 28th Int.Cosmic Ray Conf., Tsukuba (Japan)* (2003) 2225.
- [22] R.A.Mukhamedshin et al., *Proc. 28th Int.Cosmic Ray Conf., Tsukuba (Japan)* (2003) 2225.
- [23] M.H.Israel et al., *NASA Report NP-2000-05-056-GSFC*.
- [24] W.Menn et al., *ApJ* **533** (2000) 281; R.Bellotti et al., *Phys.Rev.* **D60** (1999) 052002; M.Boezio et al., *ApJ* **518** (1999) 457; T. Sanuki et al., *ApJ* **545** (2000) 1135.
- [25] S. Haino et al., *Phys.Lett.* **B594** (2004) 35.
- [26] J.Burger, *Eur.Phys.J.* **C33** (2004) 941.
- [27] V.S. Berezinskii, S.V. Buolanov, V.A. Dogiel, V.L. Ginzburg, & V.S. Ptuskin 1990, *Astrophysics of Cosmic Rays* (Amsterdam: North-Holland).

- [28] D. Maurin, F. Donato, R. Taillet, P. Salati, *ApJ* **555** (2001) 585.
- [29] D. Maurin, R. Taillet, F. Donato, *A&A* **394** (2002) 1039.
- [30] A. Wandel et al., *ApJ* **316** (1987) 676; A. Wandel, *A&A* **200** (1988) 279.
- [31] E.G. Berezhko et al., *A&A* **410** (2003) 189.
- [32] D. Maurin, M. Cassé, E. Vangioni-Flam, *Astropart. Phys.* **18** (2003) 471.
- [33] R. H. Kraichnan, *Phys. Fluids* **8** (1965) 1385.
- [34] F.C. Jones et al., *ApJ* **547** (2001) 264.
- [35] J.W. Armstrong, J.M. Cordes, B.J. Rickett, *Nature* **291** (1981) 561.
- [36] J. Scalo, B. G. Elmegreen, *Ann.Rev.Astron.Astrophys.* **42** (2004) 275.
- [37] M.Aglietta et al., *ApJ* **470** (1996) 501; T.Antoni et al., *ApJ* **604** (2004) 687.
- [38] L. O’C. Drury et al., *Space Sci. Rev.* **99** (2001) 329.
- [39] E.G. Berezhko, V.K. Yelshin, L.Y. Ksenofontov, *Astropart. Phys.* **2** (1994) 215.
- [40] F. A. Aharonian et al. (H.E.S.S. Collaboration) *Nature* **432** (2004) 75.
- [41] F. Donato et al., *ApJ* **563** (2001) 172.
- [42] F. Donato, D. Maurin, and R. Taillet, *A&A* **381** (2002) 539.
- [43] D. Maurin et al., *Research Signposts, "Recent Research Developments in Astrophysics"*, astro-ph/0212111.
- [44] B.Wiebel-Sooth et al., *A&A* **330** (1998) 389.
- [45] L.W.Howell, *Nucl.Instr. and Meth.Phys.Res.* **A480** (2002) 741.
- [46] E.Juliusson et al., *ApJ* **191** (1974) 331.
- [47] J.H.Caldwell, *ApJ* **218** (1977) 269.
- [48] F.Gahbauer et al., *ApJ* **607** (2004) 333.
- [49] R. Taillet et al., *ApJ* **609** (2004) 173.
- [50] I.Büsching et al., *ApJ* **619** (2005) 314.
- [51] J.Ahrens et al., *Astropart. Phys.* **21** (2004) 565.
- [52] The Super-Kamiokande Collaboration, Ashie Y. et al., hep-ex/0501064, *subm. to Phys. Rev. D.*
- [53] F. Donato et al., *Phys. Rev.* **D69** (2004) 063501.
- [54] A. Bottino et al., *Phys. Rev.* **D70** (2004) 015005.
- [55] F. Donato, N. Fornengo, P. Salati, *Phys. Rev.* **D62** (2000) 043003.